

## Fabrication and Structural Control of PLLA/clay Two-dimensional Nanocomposite in Organized Molecular Films

Yoshitaka Takahara, Naoya Ninomiya and Atsuhiko Fujimori\*

Graduate School of Science and Engineering, Yamagata University, Yonazawa, Yamagata 992-8510, Japan

Fax: +81-238-26-3073, e-mail: fujimori@yz.yamagata-u.ac.jp

Langmuir-Blodgett (LB) films of organo-modified montmorillonite (abbreviated as C<sub>18</sub>-clay) and poly(L-lactic acid) (PLLA) / C<sub>18</sub>-clay intercalated multilayer films formed and the structures were investigated by out-of plane X-ray diffraction (XRD), in-plane XRD, and atomic force microscopy (AFM). Intercalated multilayers were constructed by the application of the LB method to C<sub>18</sub>-clay monolayers and the horizontal lifting method to PLLA monolayers. Further, surface morphology of PLLA : C<sub>18</sub>-clay mixed Z-type monolayers on solid were also estimated by AFM.

Because these systems are two-dimensional ultrathin layer models related to polymer / clay nanocomposite as hybrid material in bulk, experimental results in this study are discussed in the view of formation mechanism and origin of functionality of three-dimensional polymer / clay nanocomposite materials, referring to the structural information of these organized molecular films.

Key words: Langmuir-Blodgett film, surface lowering method, organo-modified montmorillonite, poly(L-lactic acid), two-dimensional nanocomposite

### 1. INTRODUCTION

Since clay particles disperse uniformly in the polymer matrix in nanometer scale, the resultant polymer/clay nanocomposites (PCNs) exhibit remarkable enhancements in stability, gas barrier performance, especially in mechanical properties as compared with conventional composites.<sup>1</sup> Several kinds of preparation methods for PCNs have been reported so far. Among *in situ* intercalative polymerization, melt-intercalation, exfoliation-adsorption, and template synthesis<sup>2</sup>, melt-intercalation has been widely used in practice due to its environmental and economical advantages.

Vaia *et al.* demonstrated for the first time the possibility of direct melt intercalation of polystyrene (PS) into mica galleries,<sup>3</sup> where the kinetics of PS melt intercalation was examined as functions of processing temperature and molecular weight of PS. However, the effects of clay content and clay surfactants on the polymer melt intercalation have not yet been studied in detail. In order to explain the intercalating mechanism polymer chains into clay galleries, a deep understanding of those effects should be necessary.

Recently, we reported uniform dispersion of clay particles in biodegradable poly(L-lactide) (PLLA) due to the interaction of PLLA into clay.<sup>4</sup> In addition, the incorporation of several percentages of clay into PLLA did not change the original orthorhombic  $\alpha$ -form of the PLLA matrix at all.<sup>4</sup> The structure and properties of PLLA/organo-modified clay hybrids have also been reported elsewhere.<sup>5</sup> There were no studies on the mechanism of the melt intercalation of PLLA into clay galleries to form PLLA/ organo-modified clay hybrids, although many research groups so far have been interested in sample preparation, characterization and physical properties, especially in view of their

mechanical properties.<sup>6</sup>

Formation of intercalated structures of polymer chains in clay galleries of PCNs was not been proved directly although origin of enhancement of mechanical properties is assigned to intercalated structures.<sup>7,8</sup> Intercalation of polymer chains by melt-compounding was been concluded on the basis of low dispersion coefficient of polymers and peak shift to low angle region in X-ray diffraction profile (Fig.1).<sup>9</sup> However widening of interlayer spacing is not a direct evidence of intercalation of chains. Further, the reported regularity of layer structures of for clays in PCNs higher than neat polymer is doubtful.

Organo-modified clays used as raw material of PCNs are amphiphilic. These clay surfaces are treated by cationic long-chain compounds. Therefore, organo-modified clays can form monolayers on the water surface and

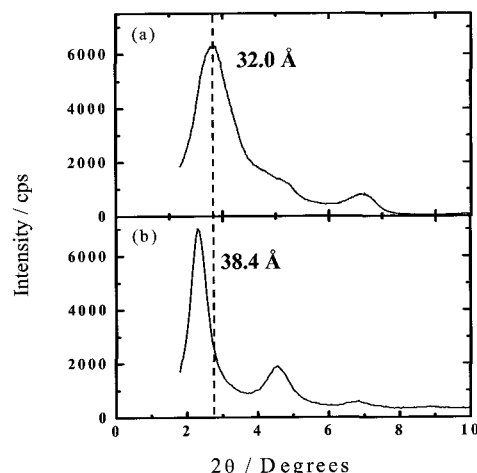


Figure 1 Wide-angle X-ray diffraction profiles of (a) clay (powder) and (b) PLLA/clay nanocomposite (clay content: 5 wt%).

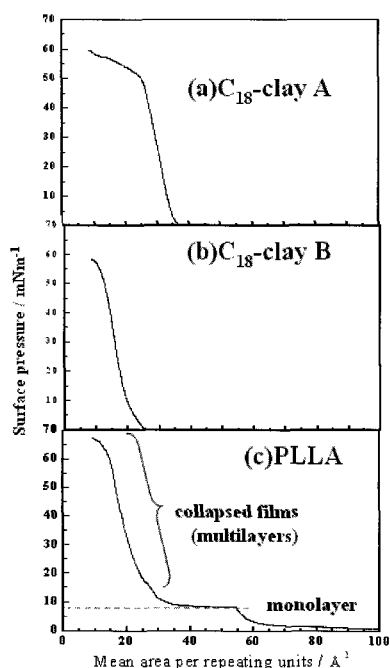


Figure 2 Surface pressure-area isotherms of organo-modified C<sub>18</sub>-clay A (a) and C<sub>18</sub>-clay A (b), and PLLA at 15 °C.

Langmuir-Blodgett (LB) films. In addition, they can form intercalated structures by applying the LB method to organo-modified clay and the horizontal lifting method to polymers. If the intercalation enhances the mechanical properties, these “intercalated molecular films” are high performance material with nanometer order the thickness at the nanometer length scale. Further, from in the viewpoint of fundamental science, it is important to prove the formation of intercalated structures in PCNs. If the intercalation alone does not enhance the mechanical properties, control of dispersion state of clay particles improve the mechanical properties by the formation of mixed monolayers.

In this study, intercalated multilayers were constructed by the application of the LB method to the organo-modified clay monolayers and the horizontal lifting method to the PLLA monolayers. Further, molecular arrangement in the LB films of two kinds of organo-modified montmorillonite (abbreviated as C<sub>18</sub>-clay A and B) and PLLA / C<sub>18</sub>-clay intercalated multilayer films was investigated by out-of plane X-ray diffraction (XRD), in-plane XRD, and atomic force microscopy (AFM). In addition, surface morphology of PLLA : C<sub>18</sub>-clay mixed Z-type monolayers was also estimated by AFM.

## 2. EXPERIMENTAL

### 2.1 Materials

Natural Na<sup>+</sup>-montmorillonite (Kunipia-F) was kindly supplied by Kunimine Co. with the cation-exchange capacity of 108.6 meq/100 g. The organophilic clay was prepared by two kinds of cation exchange reactions of natural clay (aqueous dispersion) with 20 % aqueous solution

(C<sub>18</sub>-clay A) or solid (C<sub>18</sub>-clay B) of dimethyl dioctadecyl ammonium chloride. Procedures of these organo-modified clays are described in reference.<sup>9</sup> PLLA pellets with a high L-lactide content (> 99%) were kindly supplied by Unitika Co. Ltd. The weight-average molecular weight ( $\overline{M}_w$ ), number-average molecular weight ( $\overline{M}_n$ ), and the polydispersity index ( $\overline{M}_w/\overline{M}_n$ ) were  $20 \times 10^4$ ,  $10 \times 10^4$ , and 1.94, respectively. Both the PLLA pellets and the clay were dried in a vacuum oven at 100 °C for two days and kept at room temperature in a silica gel-dried desiccator. The natural clay and organo-modified clay powder showed the interlayer spacings ( $d_{001}$ ) of 0.97 nm and 3.21 nm, respectively.<sup>9</sup>

### 2.2 Formation of organized molecular films

The organo-modified clay and PLLA were spread from toluene and chloroform solutions (approximately  $10^{-4}$  M) onto distilled water (approximately 18 M $\Omega$ ·cm), respectively. The surface pressure-area ( $\pi$ -A) isotherms were measured by a FACE film balance (Kyowa Kaimen Co.) at 15 °C. The C<sub>18</sub>-clays formed extremely condensed monolayers on the water surface (Figs. 2(a) and 2(b)). PLLA monolayers collapsed at 8 mNm<sup>-1</sup> (Fig. 2(c)). These monolayers were transferred onto glass (XRD samples) or mica (AFM samples) substrates at 15°C using the LB method in the case of C<sub>18</sub>-clays and the horizontal lifting method in the case of PLLA at 30 mNm<sup>-1</sup> and 5 mNm<sup>-1</sup>, respectively. In the case PLLA : C<sub>18</sub>-clay hybrid (mixed) monolayers, Z-type films were fabricated using the surface lowering method at 5 mNm<sup>-1</sup>.

### 2.3. Wide-angle X-ray diffraction (WAXD) of bulk powder and out-of plane X-ray diffraction of organized molecular films

The structures of the C<sub>18</sub>-clays in bulk and the layer structures of organized molecular films were characterized with a RAD-rA diffractometer (RIGAKU Co.; in the case of organized molecular films, the out-of plane X-ray diffraction method was used). Ni-filtered CuK $\alpha$  radiation (wavelength  $\lambda = 0.154$  nm) was generated at 40 kV and 100 mA. In the  $\theta$ - $2\theta$  mode, the samples were scanned by a step-scanning method with a step width of 0.05° and intervals of 4 s for the diffraction angle  $2\theta$  in the range of 2–35°. The diffracted X-ray beam was monochromatized by a pyrographite monochromatic system and

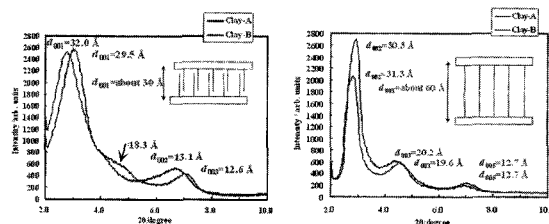


Figure 3 WAXD profiles of bulk and LB films of C<sub>18</sub>-clay A and B, respectively.

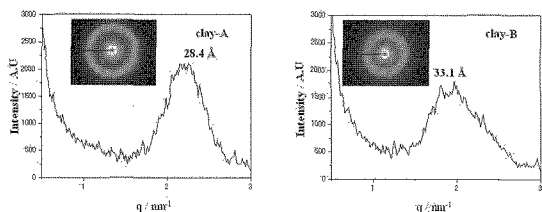


Figure 4 SAXS patterns and profiles of organo-modified clays. monitored by a scintillation counter.

2.4. Small-angle X-ray scattering (SAXS)

The crystalline morphology of the organo-modified clays was characterized with a SAXS instrument (M18XHF, MAC Science Co.) comprised of an 18 kW rotating-anode X-ray generator with a Cu target ( $\lambda = 0.154$  nm) operated at 50 kV and 300 mA. This instrument was equipped with a pyrographite monochromator, pinhole collimation system ( $\phi \sim 0.3, 0.3, 1.1$  mm), vacuum chamber for the scattered beam path, and two-dimensional imaging plate detector (DIP-220). The sample-to-detector distance was adjusted to 710 mm. The exposure time for each sample was 30 min.

2.5 Atomic force microscopy (AFM)

The surface morphologies of the transferred films were observed using a scanning probe microscope (Seiko Instrument, SPA300 with SPI-3800 probe station) using microfabricated rectangular  $\text{Si}_3\text{N}_4$  cantilevers with integrated pyramidal tips with a constant force of 0.09 N/m.

2.6 In-plane X-ray diffraction

The in-plane spacing of the two-dimensional lattice of the films was determined by analysis using an X-ray diffractometer for different geometrical arrangements (Bruker AXS, MXP-BX,  $\text{CuK}\alpha$  radiation, 40 kV, 40 mA, an instrument specially made to order) equipped with a parabolic graded multilayer mirror.

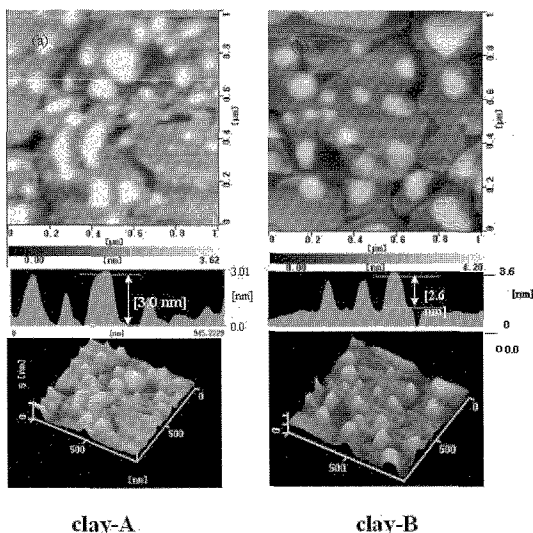


Figure 5 AFM images of Z-type monolayers of clay-A (a) and clay-B (b).

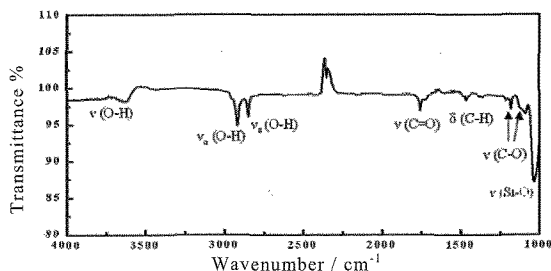


Figure 6 IR spectrum of a PLLA/clay intercalated multilayer (10/20 layers).

3. RESULTS AND DISCUSSION

Figure 3 shows the WAXD profiles for bulk state (right) and LB films (left, 20 layers) of  $\text{C}_{18}$ -clay A and B. In the bulk state, both  $\text{C}_{18}$ -clays form interdigitated structures.<sup>3, 4</sup> From the profile of  $\text{C}_{18}$ -clay B in bulk, the shoulder peak at 18.3 Å is confirmed whereas profile of  $\text{C}_{18}$ -clay A clearly has (001) and (002) peaks with no shoulders. In the WAXD profiles of the LB films of  $\text{C}_{18}$ -clay A and B, the (002), (003), and (004) reflection peaks are commonly confirmed in both cases. The comparison of peak intensity, shows that more ordered structures are formed in the LB films of  $\text{C}_{18}$ -clay A.

Figure 4 shows the SAXS patterns and profiles of  $\text{C}_{18}$ -clay A and B in bulk state. Judging from peak width of SAXS profiles, more homogeneous distribution is attained in  $\text{C}_{18}$ -clay A. Further, this agrees with the WAXD results of a slightly shorter long spacing value of  $\text{C}_{18}$ -clay A than that of  $\text{C}_{18}$ -clay B.

Figure 5 shows the AFM images of Z-type monolayers of  $\text{C}_{18}$ -clay A and B. Treatment of clays with dimethyl dioctadecyl ammonium cation does not always result in homogeneous structures. The content of organic material in  $\text{C}_{18}$ -clay A seems to be higher than that in  $\text{C}_{18}$ -clay B. On the basis of these results, we applied  $\text{C}_{18}$ -clay A as film-forming material for PLLA/clay intercalated multilayers.

Figure 6 shows an IR spectrum of a PLLA/clay intercalated multilayer (10 layers of PLLA sandwiched by  $\text{C}_{18}$ -clay A layers). Both Si-O stretching band of clay ( $1050 \text{ cm}^{-1}$ ) and C=O stretching band of PLLA ( $1740 \text{ cm}^{-1}$ ) appear in

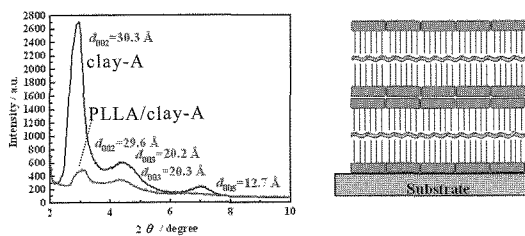


Figure 7 (left) out-of plane XRD profiles of LB multilayers for organo-modified clay and PLLA/clay intercalated films. (right) Schematic models of PLLA/clay intercalated multilayers.

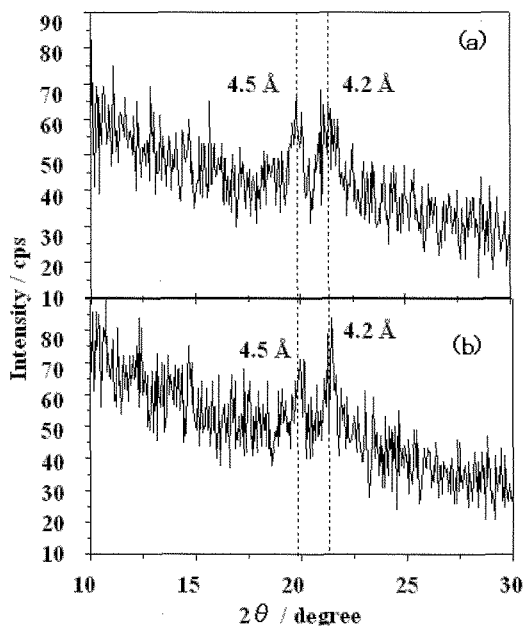


Figure 8 In-plane XRD profiles of LB multilayers (20 layers) for organo-modified clay and PLLA/clay intercalated multilayers (10/20 layers).

the spectrum. Therefore, we concluded the formation of a PLLA/organo-clay intercalated ultra thin film.

Figure 7 shows out-of plane XRD profiles of  $C_{18}$ -clay LB film and intercalated films. This result shows that peak shift to low angle side in WAXD profile does not always mean intercalation of polymer chains. The WAXD profile of the intercalated film does not exhibit peak shift, increase in intensity or narrowing of the peaks. In the film plane, the packing mode of alkyl chain of the intercalated film is the same as that of the  $C_{18}$ -clay LB film estimated by in-plane XRD measurements (Fig. 8) although regularity along the  $c$ -axis extremely decreased as shown in Fig. 7. The packing of hydrocarbons in clay surface should be orthorhombic (Fig. 9).

Figure 10 shows the AFM images of PLLA/clay hybrid Z-type monolayers at various mixing ratios. These images show the

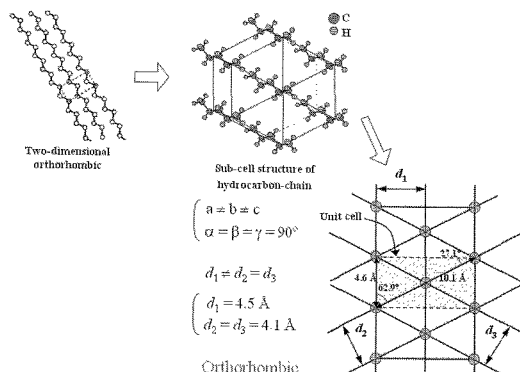


Figure 9 Schematic models of packing for alkyl chain in organo-modified clay LB films.

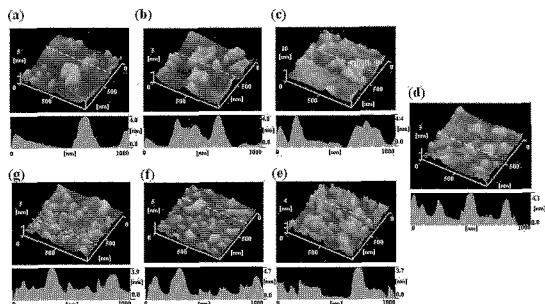


Figure 10 AFM images of PLLA : clay hybrid monolayers at various mixing ratios; (a) 5:1, (b) 3:1, (c) 2:1, (d) 1:1, (e) 1:2, (f) 1:3, (g) 1:5.

possibility to control the dispersion state of clays by the fabrication of mixed monolayers. If enhancement of mechanical properties is not related to the intercalated structures, there are many ways by which dispersion of clay particles contributes to the improvement of properties. In the near future, surface rheology of PLLA/ $C_{18}$ -clay hybrid monolayers will be estimated by the visco-elastic AFM (VE-AFM) methods. In preliminary results by VE-AFM, systematical changes in elasticity depending on the mixing ratio were observed. Enhancement of mechanical properties should be caused by not the intercalated structures but by dispersion state of clay particles in the PCNs.

## REFERENCES

- [1] P. C. LaBarton, Z. Wang and T. Pinnavaia, *J. Appl. Clay Sci.*, **15**, 11 (1999).
- [2] M. Alexandre and P. Dubois, *Mater. Sci. Eng.*, **28**, 1 (2000)
- [3] R. A. Vaia, H. Ishii and E. P. Giannelis, *Chem. Mater.*, **5**, 1694 (1993).
- [4] P. H. Nam, A. Fujimori and T. Masuko, *J. Appl. Polym. Sci.*, **93**, 2711 (2004).
- [5] N. Ninomiya, A. Fujimori and T. Masuko, *Macromol. Symp.*, **239**, 97 (2006).
- [6] M. Pluta, A. Galeski, M. Alexandre and M. A. Paul, P. Dubois *J. Appl. Polym. Sci.*, **86**, 1497 (2002).
- [7] H. R. Dennis, D. L. Hunter, D. Chang, S. Kim, J. L. White J. W. Cho and D. R. Paul, *Polymer*, **42**, 9513 (2001).
- [8] T. D. Fornes, P. J. Yoon, H. Keskkula and D. R. Paul, *Polymer*, **42**, 9929 (2001).
- [9] P. H. Nam, M. Kaneko, N. Ninomiya, A. Fujimori and T. Masuko, *Polymer*, **46**, 7403 (2005).

(Received December 5, 2007; Accepted February 15, 2008)